Electronic Supplementary Material (ESI) for Sustainable Energy & Fuels.
This journal is © The Royal Society of Chemistry 2020

Electronic Supplementary Information

Understanding of A-site non-stoichiometry in perovskites: promotion of exsolution of metallic nanoparticles and hydrogen oxidation process in solid oxide fuel cells

Na Yu,[a] Guang Jiang,[b] Tong Liu,[a**] Xi Chen,[a] Mengyu Miao,[a] Yanxiang Zhang,[b***] and Yao Wang[a*]

[a] Key Laboratory of Hydraulic Machinery Transients (Wuhan University), Ministry of Education, School of Power and Mechanical Engineering, Wuhan University, Wuhan, Hubei 430072, China

[b] National Key Laboratory for Precision Hot Processing of Metals, School of Materials Science and Engineering, Harbin Institute of Technology, Harbin 150001, China

Corresponding Authors

*Email: pmewy@whu.edu.cn (Y. W.), liu_tong@whu.edu.cn (T. L.) & hitzhang@hit.edu.cn (Y. Z.)

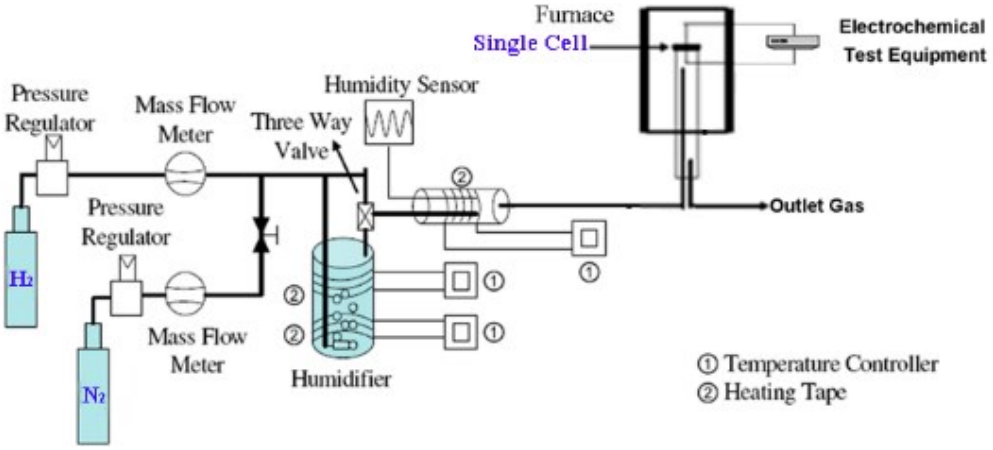

Fig. S1 Schematic diagram of the home-made setup for the measurement of the electrochemical performance of a single cell.

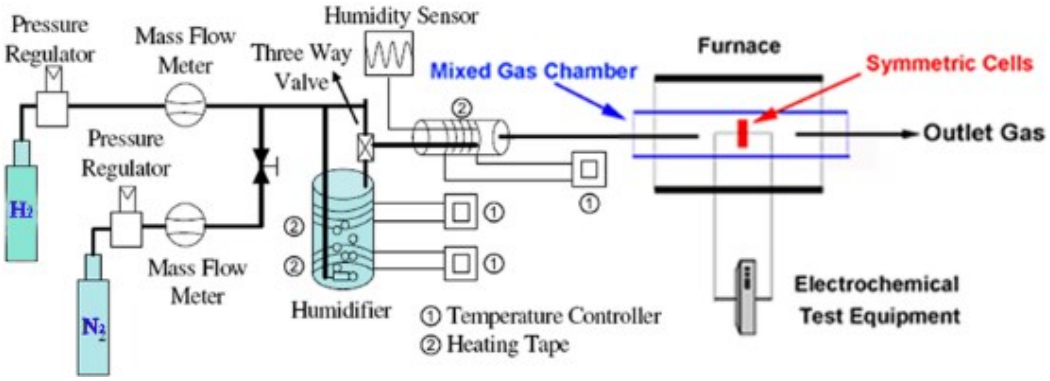

Fig. S2 Schematic diagram of the home-made setup for the measurement of the electrode polarization resistance via a symmetrical cell.

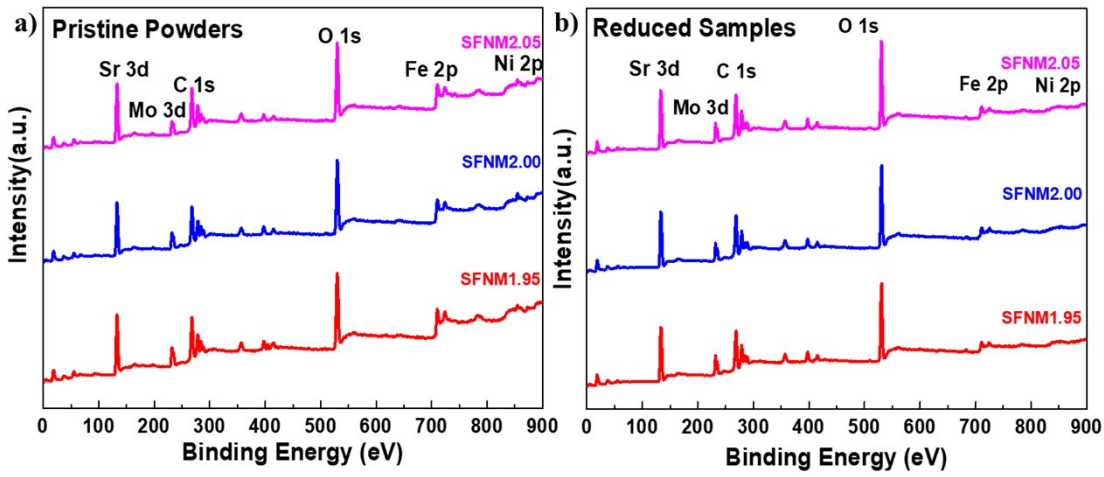

Fig. S3 XPS spectra of pristine SFNM*x* powders and reduced SFNM*x* powders (*x*=1.95, 2.00, and 2.05), a) pristine SFNM*x* powders, and b) reduced SFNM*x* powders.

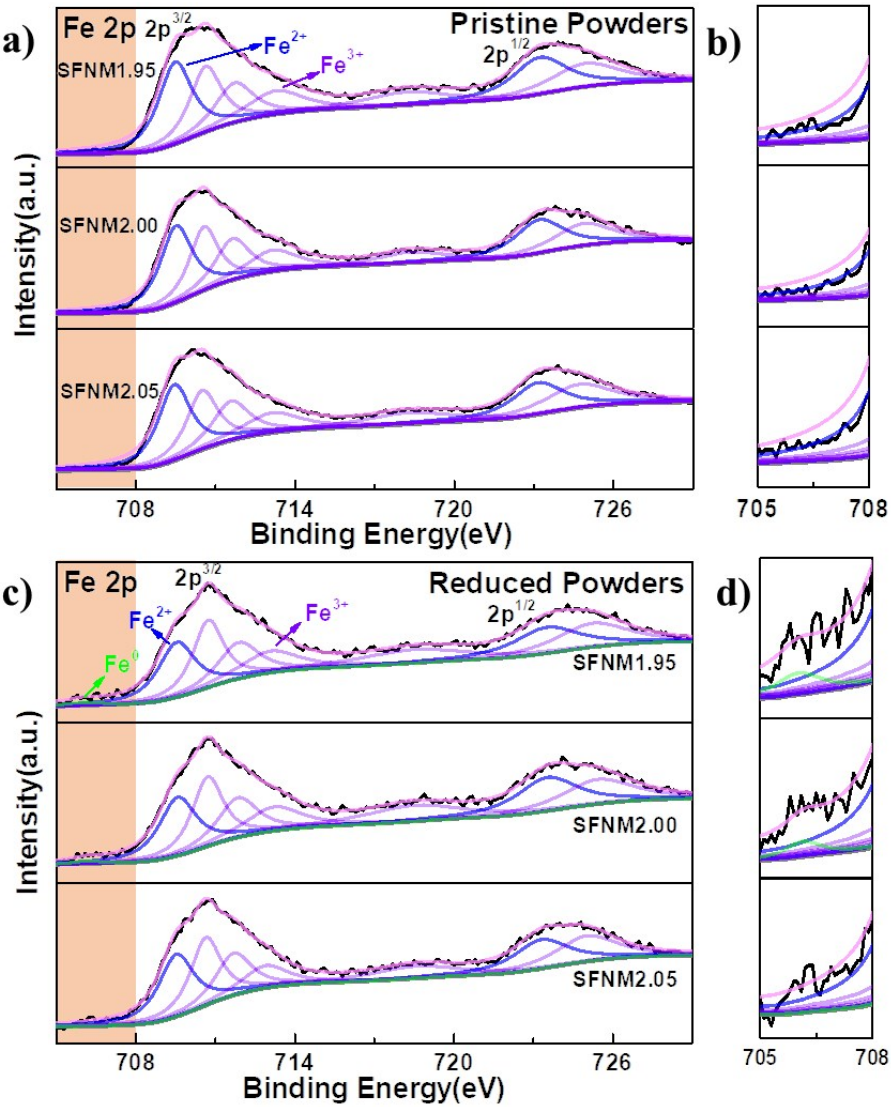

Fig. S4. XPS spectrum of Fe 2p core level regions of a-b) the pristine SFNM*x* powders and c-d) the reduced SFNM*x* powders (*x*=1.95, 2.00, and 2.05) in the banding energy range of a) and c) 705-729 eV and b) and d) 705-708 eV.

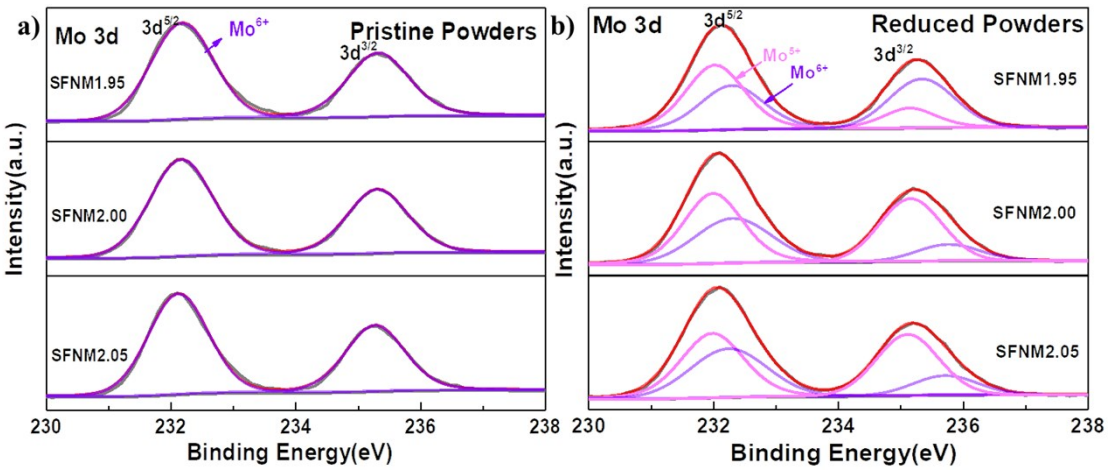

Fig. S5 XPS of Mo 3d of the core level regions of a) pristine SFNM*x* powders and b) reduced SFNM*x* powders (*x*=1.95, 2.00, and 2.05).

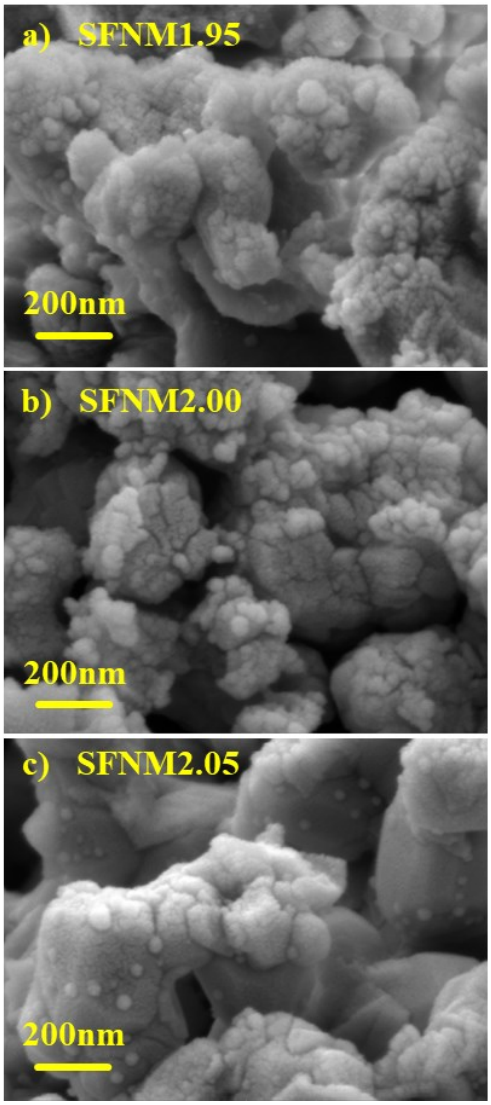

Fig. S6 Cross-sectional SEM images of a) SFNM1.95 electrode, b) SFNM2.00 electrode, and c) SFNM2.05 electrode in the symmetric cells after testing in 97%H_2-3%H_2O.

.

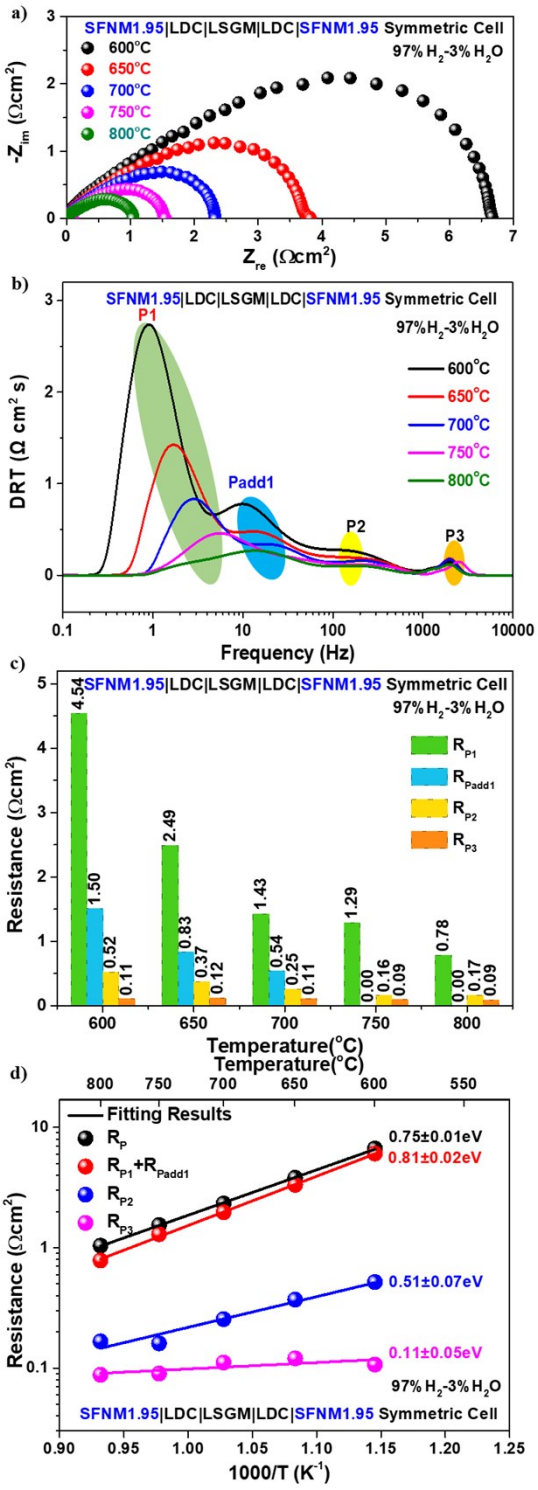

Fig. S7. a) The Nyquist plots, b) the corresponding DRT analysis results, c) resistances of the resolved peaks calculated from the DRT analysis results shown in Fig. S7b, and d) Arrhenius plots of R_ps and resistances of the resolved peaks shown in Fig. S7c of the symmetrical cell with SFMNi1.95 electrodes in 97%H_2-3%H_2O atmosphere measured at 600-800 ^oC.

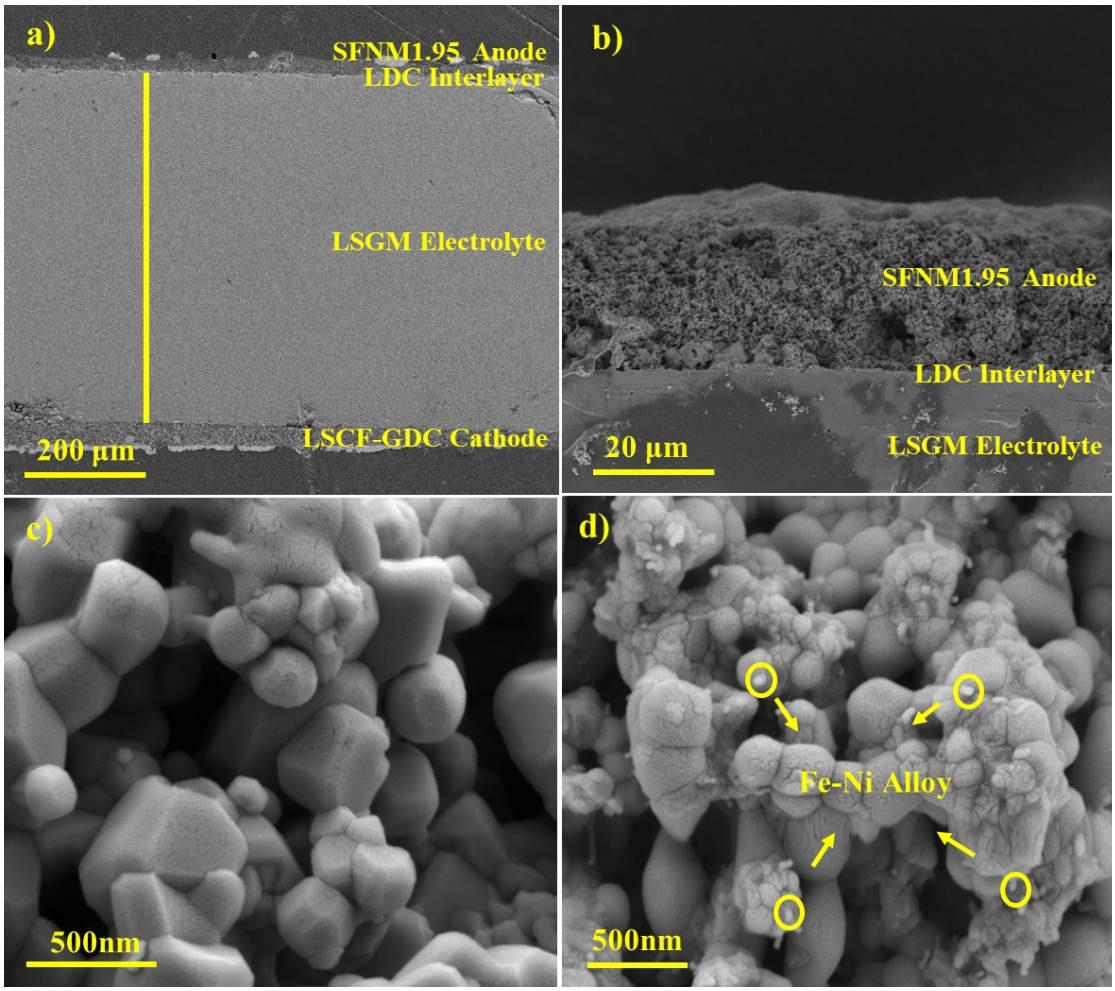

Fig. S8 Cross-sectional SEM images of a) the single cell and b) the interface of anode/interlayer/electrolyte, and SEM images of SFNM1.95 anode c) before and b) after testing.

Table S1 A table of cell performance comparison obtained with various hydrogen electrodes at 800°C using 97%H_2-3%H_2O as the feeding gas

Anode	Cathode	Electrolyte(μm)	R_p(Ωcm^2)	Ref.
SFNM1.95	LSCF-GDC	LSGM(580)	0.25	This work
Ba_2FeMoO_6(BFMO)	SCF	LSGM(300)	1.2	[64]
Sr_2FeMoO_6(SFMO)	SCF	LSGM(300)	0.91	[64]
Ni-YSZ	LSCF	YSZ(20)	0.81	[65]
$SrMo_{0.9}Ga_{0.1}O_{3-\delta}$	SCFO	LSGM(300)	0.66	[66]
$Sr_{1.9}MgMoO_{6-\delta2}$	BSCF	LSGM(280)	0.31	[50]
$Sr_2Fe_{1.5}Mo_{0.5}O_{6-\delta}$	SFM	LSGM	0.27	[71]
$La_{0.75}Sr_{0.25}Cr_{0.5}Mn_{0.5}O_{3-\delta}$	LSM	LSGM(120)	0.16	[72]
MDC infiltrated Ni-YSZ	LSM-YSZ	YSZ(30)	0.42	[69]
$La_{0.4}Sr_{0.6}Fe_{0.7}Ti_{0.1}Co_{0.2}O_{3-\delta}$ (CoFe@LSFTC-20)	LSFTC-20	LSGM(300)	1.47	[63]
$La_{0.95}Fe_{0.8}Ni_{0.05}Ti_{0.15}O_3$(Ni@LFNT)	LSC	LSGM(350)	0.51	[67]
$(NiO)_{0.05}$-$(SrTi_{0.8}Nb_{0.2}O_3$-δ$)_{0.95}$ (Ni@STN)	LSCF	LSGM(300)	0.38	[29]
$Pr_{0.8}Sr_{1.2}(Co,Fe)_{0.8}Nb_{0.2}O_{4+\delta}$ (CoFe@K-PSCFN-CFA)	P-PSCFN	LSGM(30)	0.44	[68]
$La_{1.2}Sr_{0.8}Mn_{0.4}Fe_{0.6}O_4$-GDC(Fe@LSMF)	LSCF-GDC	LSGM(280)	0.31	[70]